INVESTIGATION OF PHOTOVOLTAIC-THERMAL (PVT) COLLECTOR FOR DIRECT COUPLING WITH HEAT PUMPS: HARDWARE IN THE LOOP (HIL) AND TRNSYS SIMULATIONS

B. Chhugani[1], M. Kirchner[1], M. Littwin[1], C. Lampe[1], F. Giovannetti[1] and P. Pärisch[1]
[1]Institute for Solar Energy Research Hamelin (ISFH),
31860 Emmerthal, Germany

ABSTRACT

The presented research work is about the investigation of an uncovered, liquid-based PVT collector, which serves as a sole heat source for a heat pump system. The PV module is thermally coupled with a fin-tube heat exchanger, which enables to use energy from the sun and ambient air optimally; hence, the collector works as a good environmental heat exchanger. Within the scope of the project, a PVT Field with a heat pump has been installed and tested dynamically under hardware-in-the-loop test environment for the energy supply of a single-family house. The result shows that the performance-factor with the system can go above 3.3 during the considered winter season.

INTRODUCTION

In PVT systems, the thermal collector rear side of a PV panel gives an additional opportunity to utilise the excessive heat for low-temperature heating application and therefore with the same PV area, higher solar energy could be harvested. Standard PVT collectors can provide both electrical and thermal energy in a ratio of about 1:4 (Helbig et al., 2018). This suggests that PVT collectors could be an ideal source for a heat pump, but the matching of demand and supply is challenging to estimate. However, the offset between supply and demand during the day can easily be compensated by a thermal storage tank on the sink side or source side of the heat pump or both; but it is still more challenging to reconcile the seasonal heat generation effect from PVT collectors. One of the solutions can be a combination of PVT with ground heat exchanger or geothermal probe on the source side of the heat pump (Bertram et al., 2012; Zenhäusern et al., 2017) but all these solutions are costly. An alternative option to replace the additional source side storage is the direct coupling of PVT to heat pump, and for that, intensive investigations have been carried out in previous works (O'Dell et al., 1984; Ito et al., 1999; and Bridgeman et al., 2008), however, in all investigations, the collector design optimisation is not addressed. An ideal PVT collector for a heat pump should extract the energy from the sun and ambient air optimally, and it should work as a good environmental heat exchanger, which can become even more reliable than air source heat pumps. Hence, in the present research work, a novel PVT collector combination of PV with backside brine-to-air fin heat exchanger as a sole heat source of a heat pump has been investigated with Hardware in the Loop (HiL) test environment. HiL is an approach to simulate and to test complex real thermal systems dynamically under real-time varying environmental constraints. A limited number of publications are available about HiL for the heating sector in buildings. One of the investigations was carried out at TU Munich in HiL testbed for heating systems with ground source heat pump, and the researcher presented the energy consumption and the deviation of the testbed operation with and without HiL. The result showed a deviation of 2% for heat generation and 5% electricity consumption of the heat pump between with and without HiL (El-Baz et al., 2018).

The present paper focuses on an investigation PVT to heat pump system for the energy supply of a single-family house with HiL tests. The energetic and dynamic analysis of these tests are discussed, and the performance indicators of the heating supply system under real weather constraints are determined.

METHODOLOGY

Hardware in the Loop testbed

Figure 1 shows the simplified hydraulic scheme of HiL setup at ISFH. The energy source (PVT collectors), the heat pump (HP) and the thermal buffer storage have been operated in real-time as hardware. In contrast, energy sinks for domestic hot water (DHW) and space heating (SH) demand of the system have been dynamically simulated and emulated. The simulation of the space heating (SH) demand of a single-family house has been carried out using TRNSYS; the emulation has been executed using controlled heating/cooling circuits. LabVIEW program has been used to control tap cascades and emulates the DHW tap profiles. The interface between TRNSYS and emulators was developed using LabVIEW as a specific TRNSYS type. Consequently, to evaluate the PVT Field, metrological equipment has been installed at ISFH location (testbed) to measure wind speed, ambient air temperature, sky temperature, hemispherical radiation on collector plane and the fluid temperatures at the collector panel inlet and outlet.

DOI: 10.3217/978-3-85125-786-1-13

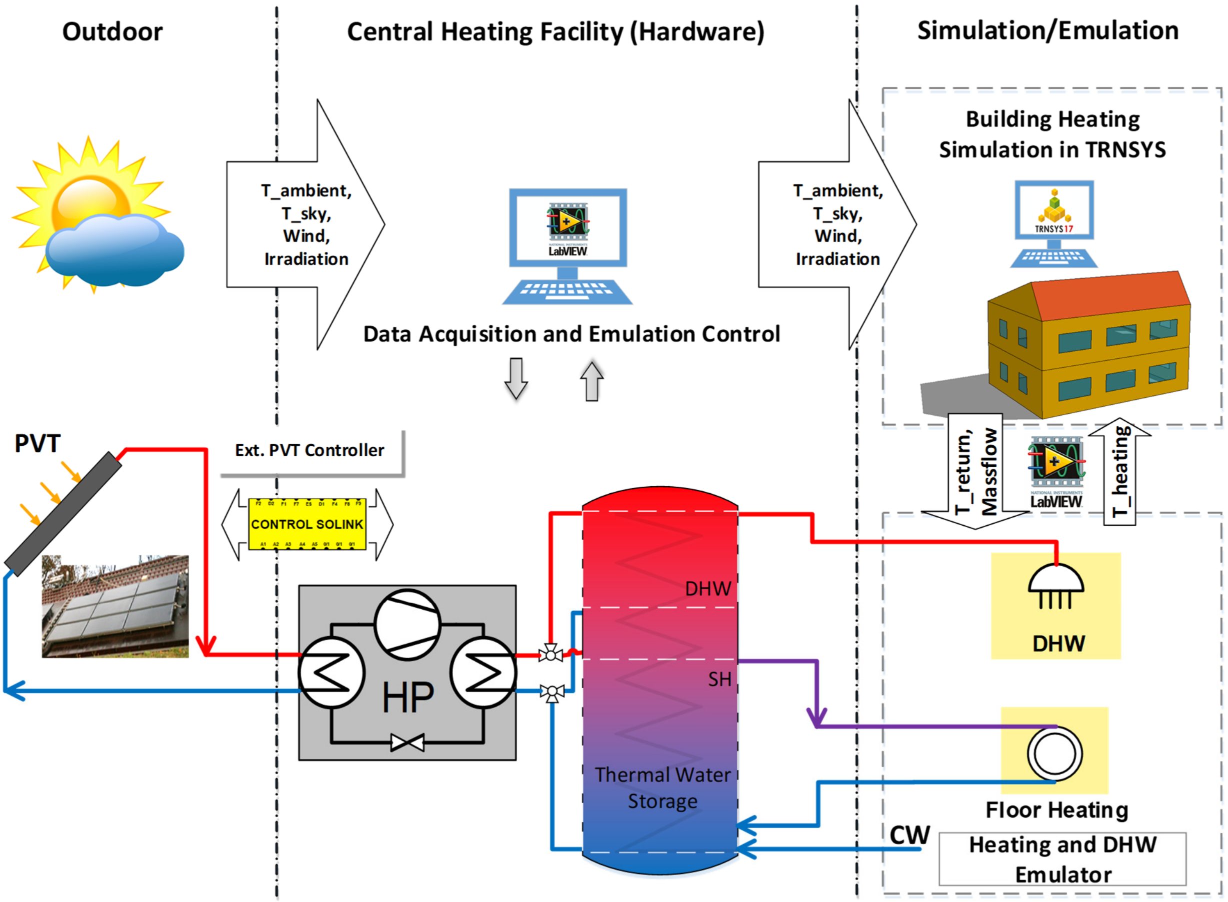

Figure 1: Simplified Hardware in the Loop (HiL) Concept at ISFH

Figure 1 shows the dynamic building simulation in TRNSYS uses the real-time measured weather data, which includes solar radiation on different surfaces of the building, sky temperature, wind speed, ambient temperature. On the other hand, for the dynamic heating simulation, the heating flow temperature is conveyed to TRNSYS, which returns the mass flow and space heating return temperature back to the emulator.

PVT collector

The PVT collector, which is used in the investigation, has been developed by the company Consolar Solare Energiesysteme GmbH, KIT and Triple Solar B.V. (Leibfried et al., 2017) and is shown in Figure 2.

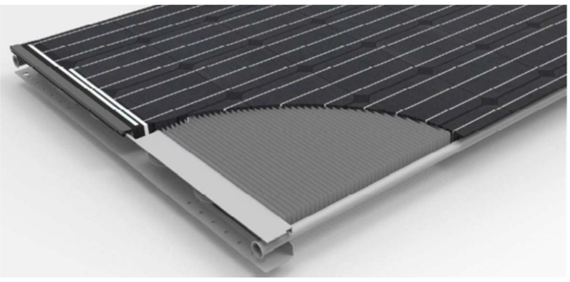

Figure 2: Sectional view of the PVT collector: the fin tube heat exchanger on the backside of the surface (Leibfried 2018)

The collector is thermally coupled with a fin tube heat exchanger, and this geometry strongly improves the performance because the fin surface is 10 times larger than the PV module area and works as an ambient heat exchanger. Hence, the surface leads to a better thermal output even in times of low irradiation. Therefore, this PVT-heat pump offers a promising alternative to conventional geothermal sources of brine-water heat pumps and can be an alternative solution to an air-water heat pump.

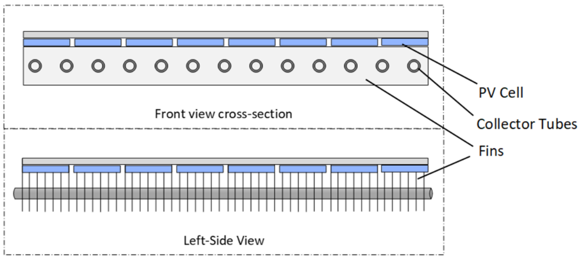

Figure 3: Schematic diagram of PVT Collector

In this PVT collector, condensation heat gains, as well as heat gains through the phase change to frost on fins surfaces improve the thermal output, which makes it particularly suitable for the low-temperature heating application. Figure 3 shows a schematic of the PVT; the heat exchanger is connected to the PV module with an adhesive layer ensuring an effective transfer of the absorbed solar energy into the fluid. The thermal efficiency of the collector was determined by means of outdoor measurements at IGTE (University of Stuttgart) according to the Standard ISO 9806 (2017) as part of a Solar Keymark certification as well as additionally investigated at the ISFH and extensively presented in (Lampe et al. 2019), and thermal collector parameter is shown in Table 1. Each module has a maximum output voltage and current of 37.6 V and 9.05 A respectively, corresponding to the maximum power output of 340 Wp under Standard Test Conditions. Within the scope of the project, nine PVT Modules with a total area of approx. 18 m² have been installed on the south-facing test roof of ISFH and monitored.

Table 1: Thermal Collector Parameter of PVT

THERMAL COLLECTOR PARAMETERS (MPP)	
η0 (collector efficiency of PVT collector)	0.468
c1 (heat loss coefficient in W/m²K)	22.99
c3 (wind dependence heat loss coefficient in J/m³K)	7.57
c4 (sky temperature dependence of the heat loss coefficient)	0.434
c5 (collector capacity in kJ/m²K)	26.05
c6 (wind dependence conversion factor in s/m)	0.067

Building

Single-Family House (SFH45) has been used as a thermal building model in the investigations. SFH45 is based on IEA SHC Task 44 / HPP Annex 38 and was developed in such a way that it can represent heating and domestic hot water demand of a new building with a good thermal insulated building envelope. The complete description of the building and boundary conditions is explained in (Dott et al., 2013), e.g. the building details such as walls, windows, ventilation, shading, internal loads. The model was adjusted and adapted in accordance with the IEA SHC & HPP T44/A38 framework during the Project "Geo-Solar-WP" for the boundary conditions of ISFH simulations in TRNSYS and documented in (Bertram 2013). In Figure 1, the simplified view of the SFH45 building model also can be seen. The building was simulated as one thermal zone model with total floor area (first and second floor) of 140 m² and internal capacities of building structures. In the model, internal walls are simplified as one 200 m² large inner walls. The total heat demand of the building is approx. 48 kWh/m²a with floor heating (thermal capacitance of 40.000 kJ/K) for the Zurich location. The tapping profile is derived from DIN EN 16147 with an energy demand of 5.845 kWh/d.

Heat pump

In the investigation, brine-water heat pump (HP) has been used with thermal power of 7.24 kW and the COP of 4.4 by B0/W35 according to the standard DIN EN 14511. This heat pump has been designed to integrate with PVT collectors as a single heat source for low-temperature heating systems; therefore, the heat pump can work up to the minimum inlet temperature of -15 °C at the evaporator side. Moreover, the heat pump has a backup electrical heater of 6 kW; however, during the investigation; the backup heater has not been used, as the heat pump has been set to monovalent operation.

Thermal water storage

The thermal combi storage has been used to supply heat and hot water to the building. It has a capacity of 560 litres with stratified charging. The storage inlets are shaped in slanted connections, with the aim to reduce thermal losses due to internal pipe circulation. An internal heat exchanger with an area of 4.1 m² heats the cold water to supply DHW. Three immersion temperature sensors have been placed over the height of the tank to assess the performance and controlling of tank temperature, as Figure 4 shows. Through these sensors set, the temperature of each layer of the tank can be well maintained and evaluated. The top and the bottom sensors measure the DHW temperature and SH temperature respectively. Both layers are heated up regularly with the heat pump. For the DHW layer, the defined temperature limit is 55 °C with -5 K hysteresis, and for the SH layer, the temperature limit is based on the heating curve from IEA SHC TASK 44 (Dott. et al., 2013) with -3 K hysteresis.

DHW and SH Emulator

The DHW emulator has been realised via three magnetic valves representing three different tapping consumers. The flow rate of the valves are adjusted manually to match the flow rate, and then the valve is controlled using LabVIEW automatically based on tapping energy profile. In this way, hot water can be drawn from the thermal tank, and the household water consumption profile can be represented.

The SH emulator primarily consists of a three-way mixing valve, temperature sensors, flow meter, PID controller, and heat exchanger. Whenever dynamic building simulations in TRNSYS demands the heating, the supply temperature is transmitted to TRNSYS via LabVIEW. The supply temperature is the actual outlet temperature from the storage tank. The TRNSYS simulated return temperature and the flow rate is adjusted in the emulator.

DOI: 10.3217/978-3-85125-786-1-13

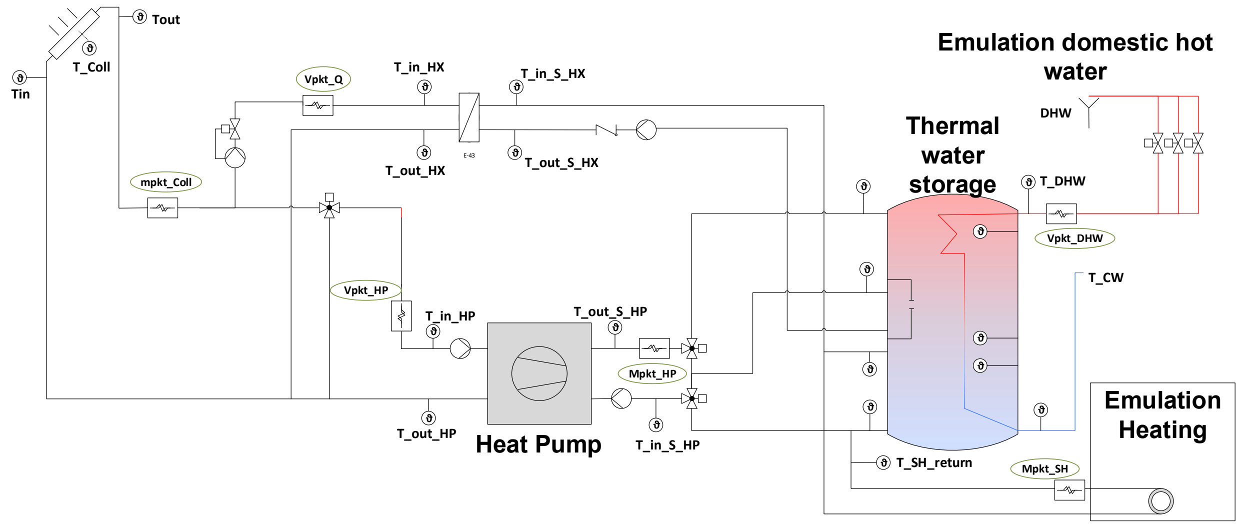

Figure 4: Detailed hydraulic schematic and measurement setup of the investigated PVT - heat pump HiL system

Monitoring and controlling

For the temperature measurement, PT100 sensors have been used, and sensor accuracy is classified according to DIN EN 60751 Class A standard with the tolerance limit of ± (0.15 °C + 0.002 T). Figure 4 shows different points, where temperatures of PVT, heat pump, thermal storage tank, emulators have been measured. Coriolis flow measurement devices were used to measure the mass flow rate at different positions.

Data acquisition was performed with an interval of a one-second time-step.

Weather

Figure 5 shows weather data such as precipitation, mean ambient temperature (T_ambient), minimum ambient temperature (T_min_ambient), solar radiation (Solar irradiance), and the wind speed near the collector plane (Wind) during measurement days

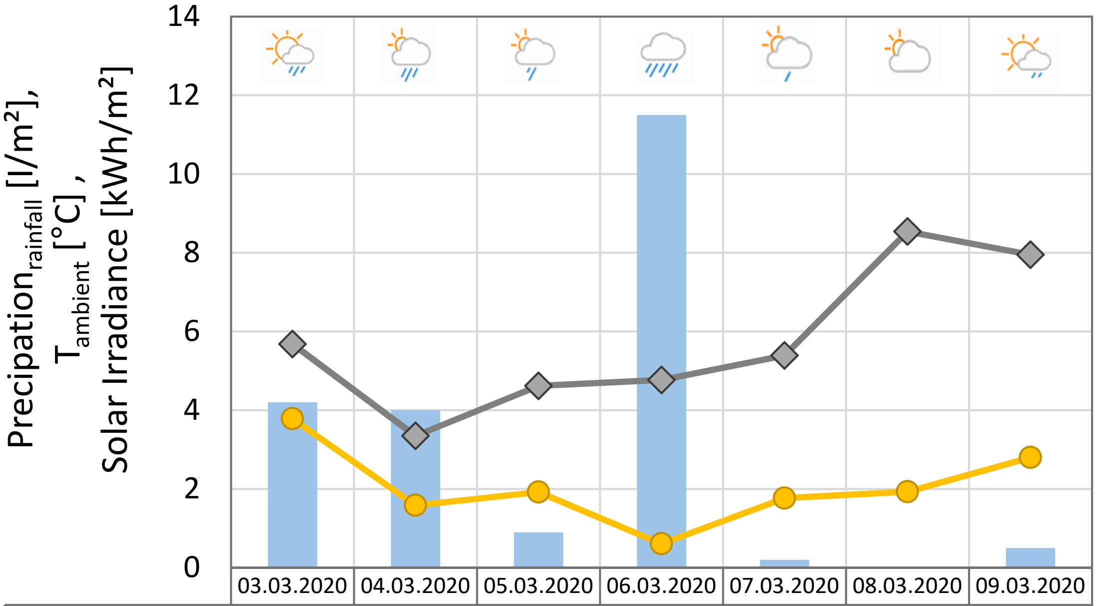

	03.03.2020	04.03.2020	05.03.2020	06.03.2020	07.03.2020	08.03.2020	09.03.2020
🟦 Precipitation	4,2	4	0,9	11,5	0,2	0	0,5
◆ T_ambient	5,7	3,4	4,6	4,8	5,4	8,5	8,0
T_min_ambient	0,8	-0,6	-1,1	2,8	1,9	4,2	5,1
● Solar irradiance	3,79	1,58	1,92	0,61	1,77	1,93	2,80
Wind	1,3	0,94	1,43	0,89	1,2	1,78	2,1

Figure 5: Weather conditions during Hardware in the Loop measurements

RESULTS AND DISCUSSION

Validation of heat sink (SH and DHW)

The initial phase of the HiL investigation aims at analysing and validating the real-time simulation and emulators. Therefore, the quantitative validation of SH demand and DHW is presented in Table 2 over investigated days. In terms of the maximum relative difference was 3.7 % for SH and 1.08 % for DHW between TRNSYS simulation and the emulation. The absolute average deviation over the one-week experiment period has detected less than 3 % for SH emulation and less than 1 % for DHW. As a result, it is proven that the emulation represents the thermal behaviour of dynamic simulated building (SH and DHW) with a good approximation.

Table 2: Quantitative system validation by comparing Hardware in the loop Simulations and Emulators

DATE	Space heating in kWh		Relative Difference %
	Emulation	Simulation	
03.03.2020	28.9	29.7	2.78 %
04.03.2020	44.1	45.5	3.12 %
05.03.2020	36.2	36.9	1.89 %
06.03.2020	44.4	45.9	3.16 %
07.03.2020	28.8	29.9	3.77 %
08.03.2020	25.7	26.2	2.02 %
09.03.2020	33.0	33.9	2.44 %
Total	**241.0**	**247.9**	**2.77 %**

DATE	DHW in kWh		Relative Difference %
	Emulation	Simulation	
03.03.2020	5.91	5.85	1.04 %
04.03.2020	5.90	5.85	0.79 %
05.03.2020	5.91	5.85	1.06 %
06.03.2020	5.91	5.85	1.08 %
07.03.2020	5.90	5.85	0.79 %
08.03.2020	5.91	5.85	1.08 %
09.03.2020	5.89	5.85	0.67 %
Total	**41.33**	**40.95**	**0.92 %**

System Performance Evaluation

As explained above, during the experiments, the system was tested with dynamic SH and DHW load; hence, for the evaluation of the system, different performance indicators were defined. These indicators are explained below in eq. 1 to 4 and the first results are presented in Figure 6. The first performance indicator is the "HPF_{SHP}" (Heating performance factor) of the system. It defines the ratio between amount of heat delivered by the system to the electrical energy consumed over a specified period. In this paper, the "HPF_{SHP}" is calculated on a daily basis. Moreover, to make a system comparable with other systems, the electrical consumption of the heating and the water circulation pump of the building is not included in the system calculation. The index is according to IEA Task - 44 SHP boundary conditions (Malenković et al., 2013).

$$HPF_{SHP} = \frac{\int (\dot{Q}_{SH} + \dot{Q}_{DHW})\, dt}{\int (\dot{E}_{HP\,+\,Pump})\, dt} \qquad (8)$$

Where, $\dot{Q}_{SH}$ is the heat delivered to space heating; $\dot{Q}_{DHW}$ is the heat delivered for domestic hot water; and $\dot{E}_{HP+Pump}$ is electricity used by the heat pump compressor and condenser/ evaporator pump.

Subsequently, the system consists of PVT collectors as a source for the heat pump; hence the generated amount of electricity from PV is also included in the performance evaluation. However, there is no battery storage in the system; therefore, only self-consumed PV electricity is included for the calculation with the energy balance based on one second time step. As a result, the second performance factor is named in eq. 2 as "HPF_{SHP-PV}", which includes the self-consumed electricity.

$$HPF_{SHP-PV} = \frac{\int (\dot{Q}_{SH} + \dot{Q}_{DHW})\, dt}{\int (\dot{E}_{HP\,+\,Pump} - \dot{E}_{PVT\_el}\,)\, dt} \qquad (2)$$

Where, $\dot{Q}_{SH}$, $\dot{Q}_{DHW}$, $\dot{E}_{HP+Pump}$ are same as explained in eq 1. $\dot{E}_{PVT\_el}$ includes the self-consumed electricity fraction by heat pump compressor and condenser, evaporator pump.

Figure 6 shows the daily heating performance factor ("HPF_{SHP}" and "HPF_{SHP-PV}") without and with direct PV consumption on the left axis, together with SH and DHW demand on the right axis during the HiL tests. In addition to that, Table 3 shows the daily average flow and return temperature for DHW and SH during HiL tests.

Table 3. Average temperatures (flow and return) on the heat sink side during measurements

DATE	DHW in °C		SH in °C	
	Flow	Return	Flow	Return
03.03.2020	51.64	12.19	30.76	22.40
04.03.2020	51.52	12.44	30.49	23.19
05.03.2020	52.61	12.54	31.43	23.09
06.03.2020	51.80	12.42	31.15	22.64
07.03.2020	51.50	11.85	31.57	22.72
08.03.2020	51.81	11.76	31.28	22.18
09.03.2020	51.62	12.18	30.76	22.40
Average	**51.79**	**12.20**	**31.06**	**22.66**

As Figure 6 shows, the system performance (HPF_{SHP}) usually remained above 3.2 with an average of 3.3, except one incident, where it dropped below 3 (04.03.2020).

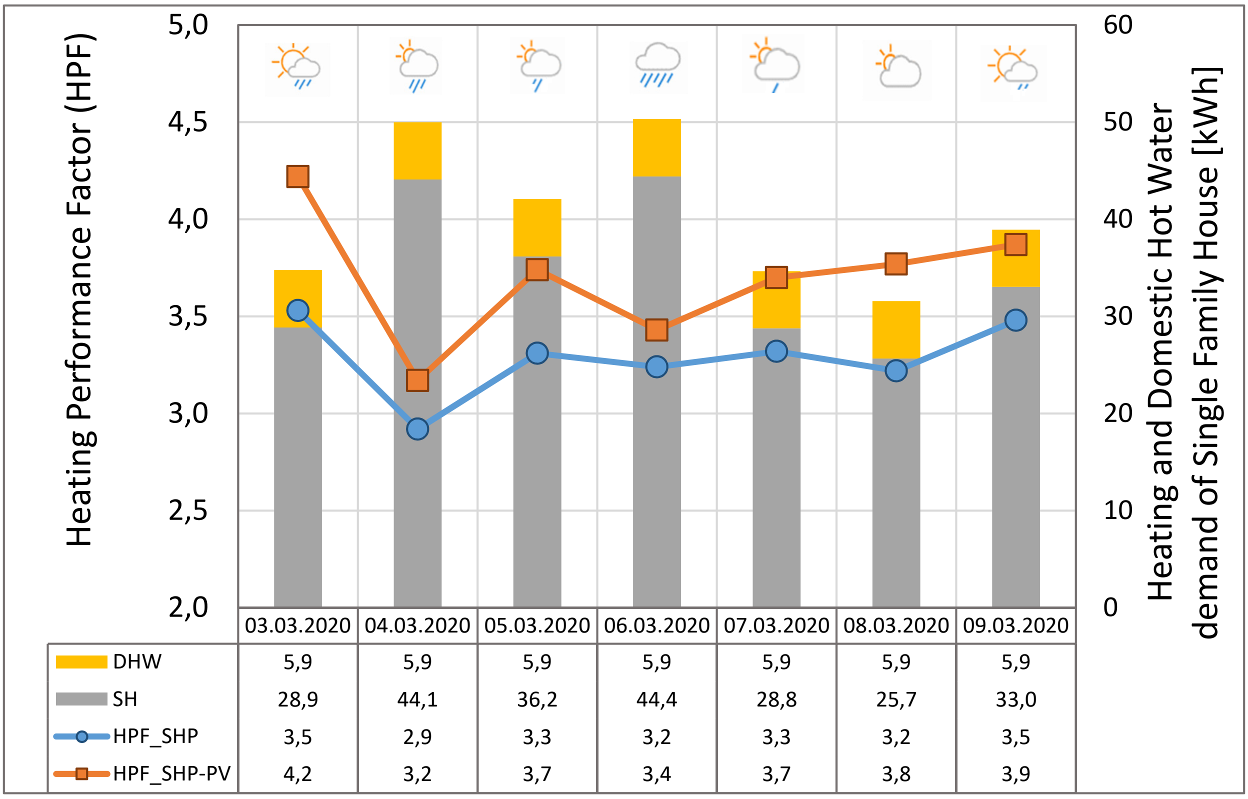

	03.03.2020	04.03.2020	05.03.2020	06.03.2020	07.03.2020	08.03.2020	09.03.2020
DHW	5,9	5,9	5,9	5,9	5,9	5,9	5,9
SH	28,9	44,1	36,2	44,4	28,8	25,7	33,0
HPF_SHP	3,5	2,9	3,3	3,2	3,3	3,2	3,5
HPF_SHP-PV	4,2	3,2	3,7	3,4	3,7	3,8	3,9

Figure 6: Daily heating performance factor of Hardware in the Loop measurements

This is due to the fact that the average mean ambient temperature was 3.4 °C, which was the lowest compared to other measuring days, and the minimum temperature fell below 0 °C with little solar radiation. Hence, the heat demand was high on that day with almost 50 kWh.

As specified before, the focus of the paper and the HiL experiment was to estimate the performance of PVT-heat pump system under representative weather conditions. As a consequence, on a cold sunny day (03.03.2020) with slight rain, the HPF_{SHP} of the system during the experiment reached 3.5 and utilised the maximum solar thermal energy in a very efficient way. Also, during the same day, the system performance including self-consumed PV electrical energy improved by 0.7 and “HPF_{SHP-PV}” increased to 4.2 due to the high solar radiation on the collector plane (67.4 kWh on the total area of 17.8 m²).

On the contrary, during a rainy day (06.03.2020) with approx. 11 litre/m² of precipitation and almost no direct solar irradiation, the system also worked very well with a performance factor of 3.2; hence, this can also prove that under these conditions the PVT collector can work as an effective environmental heat exchanger.

In this research work, PVT collector is used with the heat pump system, and the heat pump can work with minimum inlet temperature up to -15 °C on the evaporator side and considered as a low-temperature heating application. Hence, the performance factor of the heat pump before storage (HPF_{bst}) would also be relevant for the system evaluation. The HPF_{bSt} is derived according to TASK 44 (Malenković. et. al., 2013) and explained in eq. 3. It represents the total heat generation from the heat pump to the electrical energy consumed by the heat pump compressor and condenser/evaporator pump.

$$HPF_{bSt} = \frac{\int \dot{Q}_{HP}\ dt}{\int \dot{E}_{HP\,+\,eva\_Pump}\ dt} \qquad (3)$$

Where, $\dot{Q}_{HP}$ is heat generation from heat pump; $\dot{E}_{HP+Pump}$ is electricity used by the heat pump compressor and evaporator pump

The result of HPF_{bSt} during HiL measurements shows table 4. The average performance factor was perceived 3.65 during the measurements.

The next performance indicator is used to evaluate the PVT collectors, as a source for the heat pump is the solar fraction (SF). This can be expressed in two different ways: the thermal fraction "$SF\_\mathrm{PVT_{thermal}}$" and the electrical fraction "$SF\_\mathrm{PVT_{electrical}}$" excluding the heating and hot water circulation pump energy.

The thermal fraction ($SF\_\mathrm{PVT_{thermal}}$)is useful in order to evaluate the PVT thermal fraction, where the solar heat goes parallel to heat pump directly on the sink side. Nevertheless, in this present work, only PVT is coupled as a heat source for the heat pump system (in series); thus, this indicator is not presented in the scope of this paper. The indicator "$SF\_\mathrm{PVT_{electrical}}$" is the ratio between electrical energy produced by PV collector to the self- consumption by the system and is shown in eq. 4. The self-consumption varies from system to system, depending on how the system boundary is defined. In this investigation, only self-consumed electricity by the heat pump is considered and calculated with the energy balance of the one-second time step. Hence, this indicated factor cannot exceed 1 because the maximum use of electricity from PVT for the heat pump is $\dot{E}_{PVT} \leq \dot{E}_{HP\,+\,Pump}$, the excess generated electricity from PV is fed to the grid.

$$SF\_\mathrm{PVT}_{\mathrm{electrical}} = \int \frac{\dot{E}_{PVT}}{\dot{E}_{HP\,+\,Pump}} dt \qquad (4)$$

Where, $\dot{E}_{PVT}$ is electricity generation from PVT; and $\dot{E}_{HP+Pump}$ is the same as explained in eq 1.

Table 4: Performance factor of Heat Pump and self-consumption PV electrical energy during HiL measurement

DATE	HPF_{bSt}	$SF\_\mathrm{PVT}_{\mathrm{electrical}}$ **(%)**
03.03.2020	3.76	16.26 %
04.03.2020	3.35	8.08 %
05.03.2020	3.58	11.47 %
06.03.2020	3.67	5.57 %
07.03.2020	3.58	10.18 %
08.03.2020	3.70	14.68 %
09.03.2020	3.92	10.06 %
Average	**3.65**	**10.90 %**

The self-consumption varies from system to system, depending on how the system boundary is defined. In this investigation, self-consumed electricity is considered only for the heat pump and as mentioned above, calculated with the energy balance of one-second time step. The total electricity consumption of the system within a period of one week was reduced by approx. 11 % with self-consumption of PV electrical energy. However, the self-consumption fraction can be increased by changing the boundary conditions of the system, i.e. by including household electricity consumption, or by integrating battery storage.

CONCLUSION

In the paper, a PVT coupled heat pump system is investigated with HiL real-time test environment. The goal of the investigation is to analyse and evaluate the system for the energy supply of a single-family house under dynamic weather conditions. Hence, PVT collector, heat pump, and buffer storage have been installed as hardware, whereas dynamic load (space heating and domestic hot water) were simulated in TRNSYS and emulated. Throughout the investigation, simulations and emulation were validated, and the result showed good agreement: the deviation between simulation and emulation was less than 3 % for SH and less than 1 % for DHW. Based on the validated system, further HiL experiments were carried out, and performance indicators were identified and discussed.

The following points summarise the essential findings and performance indicators:

- The mean heating performance factors HPF_{SHP} and HPF_{SHP-PV} were observed 3.3 and 3.7 respectively through the measuring period of 7 days in winter
- During the sunny winter day, higher solar energy could be harvested from PVT with HPF_{SHP} of 3.5, and at the same time performance factor including self-consumed electricity was increased to 4.2
- For the rainy and cloudy day, the PVT collector acted as a good environmental heat exchanger thanks to the 10 times larger fin area than the PV surface and HPF_{SHP} values reached above 3.2
- The average self-consumed electricity fraction from PVT through the HiL experiment was approx. 11 %. This could be increased further by implementing a PV oriented control strategy.

Overall, when the investigated PVT collectors are directly coupled with the heat pump as a sole source (thermal side), the achieved system efficiency is good and can be used as a noise-free alternative to an air source heat pump. Also, by considering PV electrical generation, the system performance factor was increased significantly.

In the next phase of the project, the system will be investigated under higher building load with higher heating and domestic hot water demand. Further HiL tests will be carried out under different/extreme conditions such as with snow-covered PVT. Additional investigations will focus on the demand-oriented system control to exploit the potential of PVT as both thermal and electrical source.

Finally, the work confirms the advantages of the HiL tests as a flexible and time-saving approach to evaluate complex energy supply systems in the building sector under real boundary conditions. The HiL tests can also include many complex systems such as PVT with ice storage.

ACKNOWLEDGEMENT

The presented work and the results are part of the research project "TwinPower - 0325867B", which is funded by the German Federal Ministry of Economy and Energy (BMWi), and supported by the Lower Saxony Ministry of Science and Culture. The authors are grateful for the support and responsible for the content of the publication.

REFERENCES

Bertram, E., Glembin, J., Rockendorf, G., 2012. Unglazed PVT collectors as an additional heat source in heat pump systems with borehole heat exchanger. IEA, International conference on Solar Heating and Cooling (SHC) for Buildings and Industry in San Francisco, USA

Bertram, E., 2013. Annex F to Report C3 of the IEA SHC Task 44 / HPP Annex 38, Platform independence checks reported for T44A38 (Report of Subtask C Nr. Adaption for the IEA SHC & HPP T44/A38. Boundary Conditions of ISFH Simulations in TRNSYS).

Bridgeman, A., Harrison, S., 2008. Experimental evaluations of Indirect Solar Assisted Heat Pump System for Domestic Water Heating. Proceedings EuroSun- 1st International Congress on Heating, Cooling and Buildings, Lisbon, Portugal.

Dott, R., Haller, M.Y., Ruschenburg, J., Ochs, F., Bony, J., 2013. The Reference Framework for System Simulations of the IEA SHC Task 44 / HPP Annex 38: Part B: Buildings and Space Heat Load, A technical report of subtask C Report C1 Part B.

El-Baz, W., Mayerhofer, L., Tzscheutschler. P., and Wagner, U., 2018, Hardware in the Loop Real-Time Simulation for Heating Systems: Model Validation and Dynamics Analysis.

El-Baz, W., Tzscheutschler, P., Wagner, U., 2018. Experimental study and modeling of ground-source heat pumps with combi-storage in buildings.

Giovannetti, F., Lampe, C., Kirchner, M., Littwin, M., Asenbeck, A., and Fischer, S., 2019. Experimental investigations on photovoltaic-thermal arrays designed for the use as heat pump source. International Solar Energy Society (ISES) Solar World Congress (SWC) 2019 in Santiago, Chile.

Helbig, S., Kirchner, M., Giovannetti, F., Lampe, C., Littwin, M., Kastner. O., 2018. PVT-Kollektoren als bisolare Wärmepumpenquelle Ein Simulationsvergleich zwischen Polysun und TRNSYS. Symposium Thermische Solarenergie Juni 2018 Bad Staffelstein.

Ito, A., Miura, N., Wang, K., 1999. Performance of a heat pump using direct expansion solar collectors. Solar Energy, 65, 3, 189-196.

Lampe, C., Kirchner, M., Littwin, M., Giovannetti, F., Asenbeck, S., Fischer, S., 2019. Experimentelle Untersuchungen an Testfeldern mit SOLINK photovoltaisch-thermischen Kollektoren. Proceedings Symposium Solarthermie und Innovative Wärmesysteme 2019, Bad Staffelstein, Germany.

Leibfried, U., Wagner, A., Abdul-Zahra, A., 2017. Schlussbericht: Hocheffiziente, auf intelligenter Verknüpfung von PVT- und Wärmepumpentechnik basierende Wärmeversorgung für Gebäudebestand und Neubau. Teil 1: Funktionsentwicklung und Aufbau eines Anwender-Konsortiums.

Leibfried, U., 2018. SOLINK PVT Energieversorgungssysteme für Wärmepumpen. Proceedings Symposium Solarthermie 2018, Bad Staffelstein, Germany.

Lipp, J.P., 2015. Flexible Stromerzeugung mit Mikro-KWK-Anlagen.

Malenković, I., Pärisch, P., Eicher, S., Bony, J., Hartl, M., 2012. Definition of Main System Boundaries and Performance Figures for Reporting on SHP Systems, Deliverable B1, IEA SHC Task 44/ HPP Annex 38.

O'Dell, P., Mitchell, J. W., Beckman, W. A., 1984. Design model and performance of heat pumps with refrigerant filled solar collectors. Journal of Solar Energy, 106, 159- 164

Zenhäusern, D., Bamberger, E., Baggenstos, A., 2017. PVT Wrap-Up: Energiesysteme mit Photovoltaisch Thermischen Solarkollektoren. Institut für Solartechnik SPF

DOI: 10.3217/978-3-85125-786-1-13